Testing the viability of measuring intraocular pressure using soundwaves from a smartphone

Soanes, Matthew; Essa, Khamis; Butt, Haider

DOI:
10.1002/eng2.12355

Received: 16 September 2020 | Revised: 9 December 2020 | Accepted: 10 December 2020

DOI: 10.1002/eng2.12355

RESEARCH ARTICLE

WILEY

Testing the viability of measuring intraocular pressure using soundwaves from a smartphone

Matthew Soanes[1] | **Khamis Essa**[1] | **Haider Butt**[1,2]

[1]School of Engineering, University of Birmingham, Birmingham, UK

[2]Department of Mechanical Engineering, Khalifa University, Abu Dhabi, UAE

Correspondence
Matthew Soanes, School of Engineering, University of Birmingham, Edgbaston, Birmingham B15 2TT, UK.

Abstract

Early detection of increasing values of intraocular pressure (IOP) due to glaucoma can prevent severe ocular diseases and ultimately, prevent loss of vision. Currently, the need for an accurate, mobile measurement of IOP that shows no correlation to central corneal thickness is unmet within the modern healthcare practices. There is a potential to utilize soundwaves as a mobile measurement method and therefore, the relationship between IOP and the reflection coefficient of sound waves is investigated. Simulations are conducted using COMSOL Multiphysics to provide theoretical confirmation of the worthiness of the experiment. An experiment is conducted to further investigate the relationship between the internal pressure of an object and its acoustic reflection coefficient. The experiment exploits the use of hydrostatic pressure to determine internal pressure, and the reflection coefficient is measured and analyzed. An initial experiment is conducted to identify the resonant frequency of the object and the optimal frequency for maximizing reflection. The experiment shows comprehensively that there is a relationship between the internal pressure of an object and its acoustic reflection coefficient, providing a confirmation of the theory that would allow mobile measurements of IOP to be conducted with the use of a smart phone.

KEYWORDS

acoustic reflection coefficient, glaucoma, intraocular pressure, ocular hypertension

1 | INTRODUCTION

The human eye is a very sensitive and cherished organ for its unparalleled use for humans on a daily basis. Thus, its continued state of health is of upmost importance to individuals worldwide. Some of the most common eye related diseases are often avoidable and display strong risk factors some time before their onset. For example, in the case of diabetic retinopathy, individuals with diabetes are specifically at risk and so are constantly monitored for background retinopathy, tiny bulges that develop in the blood vessels of the eye.[1] However, in the case of glaucoma, an ocular disease with age and elevated levels of intraocular pressure (IOP) as significant risk factors, it is harder to specify such a specific group of individuals at risk of development. For this reason, an accurate, non-invasive, mobile measurement of IOP would provide a means to continuously monitor an individual's IOP over an extended period. This would lead to earlier diagnosis and treatment of the condition, drastically increasing the chances of maintaining the individual's vision.

The discussed methods will identify if an individual has an elevated IOP, however individuals can still develop normal tension glaucoma, or have an inflated IOP (ocular hypertension) and not develop glaucoma. It is important to note therefore, that the methods will not directly diagnose an individual with glaucoma, however serve an important purpose in detecting a large risk factor in the disease's development. There are also other risk factors that are important in the development of glaucoma, such as intracranial pressure or cerebrospinal fluid pressure. Intracranial pressure is the pressure inside the cranium, and the cerebrospinal fluid pressure being the pressure throughout the neuraxial system more generally. The two are directly correlated, and thus, are used interchangeably. They have both been shown to be independent, significant risk factors in the development of glaucoma, proved in both the presence and absence of an elevated IOP level.[2-4] In addition, simulations have indicated that intracranial pressure has been shown to play a significant role in post-laminar neural tissue failure, causing damage to the eye.[5]

IOP, however remains as a vital measurement in the continued healthy state of the human eye. It is defined as "the pressure created by the continued renewal of fluids within the eye",[6] where a healthy value between 10 and 20 mmHg is essential to maintain the conditions for optimal refraction.[7] Ocular hypertension is caused by an imbalance in the production and drainage of aqueous fluid in the eye. This imbalance is most common in older adults, with the risk increasing as the individual gets older and in turn, increasing the risk of the individual developing Glaucoma. Glaucoma is a disease of the optic nerve which affects 64.3 million people worldwide as of 2013,[8] if left untreated it causes irreversible damage to the nerve and loss of sight. The difference between a healthy eye and a glaucoma-inflicted eye is shown in Figure 1.

The current, 'gold standard' method of measurement of IOP is applanation tonometry,[9] namely Goldmann (slit lamp) or Perkins (handheld), as illustrated in Figure S1a and S1b. This works on the Imbert-Fick law, which states that "the force required to flatten or applanate a sphere (W) is equal to the product of the pressure inside the sphere (P) and the area applanated (A): $W = P \times A$".[10] In practice, numbing drops followed by non-toxic dye are applied to the patient's eyes. This provides the base for the measurement which is gathered by a small tip indenting a small area of the cornea,[11] and the required force for this measured. Although this is considered 'gold standard', it does arise with problems and in turn, errors in measurement.

An independent risk factor of glaucoma is having a thin central corneal thickness (CCT),[11] which is a transparent layer forming the front of the eye. This can be caused by natural occurrence, or a common procedure like laser eye surgery. However, a thin CCT also causes artificially low readings of IOP when using applanation tonometry,[9] which has been recorded as a difference of as much as 0.32 mmHg per 10 μm change in CCT.[10] The only way to decipher whether the reading is artificial, or healthy and correct is by a full eye examination including a measurement of CCT, rendering an isolated, mobile applanation measurement of IOP (Perkins) useless. Furthermore, a Perkins tonometer is too expensive to be accessible for purchase by the majority of the population for home usage for prolonged IOP monitoring.

Even a Goldmann-type tonometer reading of IOP can cause large errors, found experimentally to be as much as 5 mmHg.[12] Considering the cut-off level of IOP that differentiates normal and abnormal is widely considered 21 mmHg, this equates to a 23.8% error, which is unacceptable.[12]

Pneumotonometry is another applanation method of measuring IOP which is less influenced by CCT and is non-contact.[9] An experiment shows there was no 'statistically significant differences in IOP as a function of change in corneal thickness or change in corneal curvature'.[13] It utilizes a floating pneumatic sensor that touches the cornea and records a measurement of IOP.[14] Usually slightly lower than Goldmann, provided the Goldmann measurement is not artificially low. In a professional setting, these values should still be treated cautiously.

A pneumotonometry form of IOP measurement is air-puff tonometry, Figure S1c, which utilizes a rapid air pulse to applanate the cornea. When this is done, an infrared light beam is reflected off the flattened surface of the cornea.[14] In essence this is a similar method as applanation, however, it achieves a measurement without the need for contact with the eye and, therefore, the numbing drops or dye. Air-puff tonometry is considered less accurate as it gives a higher reading of IOP in 74% of patients, as shown by experimental evidence.[14] It is also considered 'uncomfortable' and 'unpleasant' by

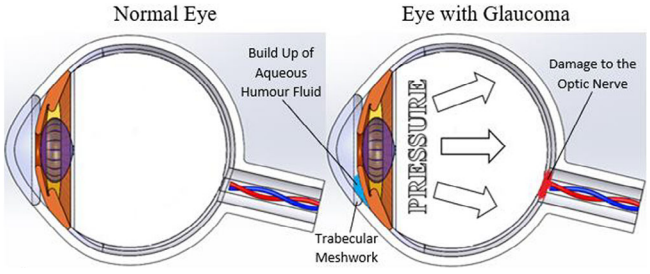

FIGURE 1 Comparison between a healthy eye and an eye suffering with glaucoma

some patients.[15] For these reasons, experiments are being conducted in to non-invasive forms of IOP measurement such as the use of ultrasound surface wave elastography or ultrasound vibro-elastography. Although these methods have been proven in a novel fashion, it is not a viable mobile method due to the machinery requirement and expertise needed to perform the measurement, thus not able to fill this gap in the market.[16,17]

As well as problems of discomfort and invasion, the diurnal fluctuation is the varying of IOP throughout the course of a single day and is caused by hormonal effects on the eyes.[18] This, in turn, causes problems in ensuring accurate measurement. Generally, IOP is higher in the morning for any one individual however the level of increase cannot be calculated. Therefore, for an accurate measurement to be taken, hourly measurements must be taken to monitor the range of the diurnal fluctuation throughout the day. This is very impractical for the discussed methods, as they must all be completed externally at an optician's and completed by a professional. For an accurate daily measurement to be taken practically, a simple, mobile measurement must be available, of which there is only one method currently in use, rebound tonometry.

Rebound tonometry, Figure S1d, is employed as a method that is 'well tolerated and safe',[19] so is suitable for children and pets. It is undertaken by a handheld device so it can be used in homes and does not require anesthetic or staining dye. It works via a tiny plastic ball being fired rapidly at the cornea, and its deceleration when they come in to contact correlating to a recorded IOP. The larger the deceleration, the higher the IOP. The plastic ball is attached to the end of a stainless-steel wire and held in place by an electromagnetic field until released.[20] However, initial experiments show that although it is a weak correlation, it shares a similar relationship with the CCT with that of Goldmann applanation tonometry, which can result in artificially low values as previously discussed. It also requires the instrument to be kept upright and kept at the correct distance from the cornea, therefore mobile measurements can prove problematic.[21] Similarly to the Perkins tonometer, a rebound tonometer is very expensive with prices starting at £1595.[22]

Another form of tonometry is being developed which looks to use a smartphone to measure IOP, and in preliminary testing, this shows a correlation to the gold-standard tonometers. Although impressive and will allow a cheap, mobile measurement to be conducted, the methods correlation with CCT will still remain a large barrier to the methods long-term application in revolutionizing the industry.[23] Another experiment has been conducted to apply fixed-force applanation in combination with a machine learning algorithm to allow a smartphone to measure IOP. Similarly to other discussed methods, this again measures 'success' by its correlation to measurements from Goldmann tonometer's, and thus, a correlation to CCT.[24]

It can be seen through this discussion of current methods, and methods which are under investigation, that a method that fits all of the criteria of being mobile, accurate, accessible and importantly, showing no correlation to an individual's CCT is not yet available.

The improved, mobile method being proposed will involve a simple procedure of firing sound waves at the eye from a predefined incident angle and measuring the coefficient of reflection. It will be conducted using a smartphone, which is widely accessible with over half of 65+ adults in America already owning one, a figure which will only increase in the future as the current population grows older (50–64, 79% ownership, 65+, 53% ownership).[25] In contrast to the previously discussed methods, it would be accessible, comfortable and simple to perform mobile readings. Furthermore, as this method does not applanate the surface of the eye CCT should not have any effect on the reflection coefficient. With all these factors taken into consideration, if the method is implemented, it will be far superior to any of the current methods of IOP measurement.

2 | MODELING

The experiment proposed will investigate if the internal pressure of an eye-replicating object affects the reflection coefficient of acoustic waves. To validate the worthiness of experimentation, modeling software COMSOL Multiphysics was utilized to prove a basic relationship between the reflection coefficient and IOP of the eye. COMSOL is used as it is a validated and trusted simulation software for reflection coefficient simulations.[26]

2.1 | Model construction

The model was constructed using a computational geometry to simulate an average human eye. Table 1 shows the geometry used for the simulation model and is based on an average between male and female values from literature. The 2D model is illustrated in Figure 2(A). A 210° revolution image of the model is shown in Figure 2(B).

TABLE 1 Simulation model geometry

Parameter	Value (mm)
Diameter	11.71[27]
Horizontal corneal curvature	7.87[28]
Thickness of cornea	0.55[28]
Thickness of precorneal tear film	0.005

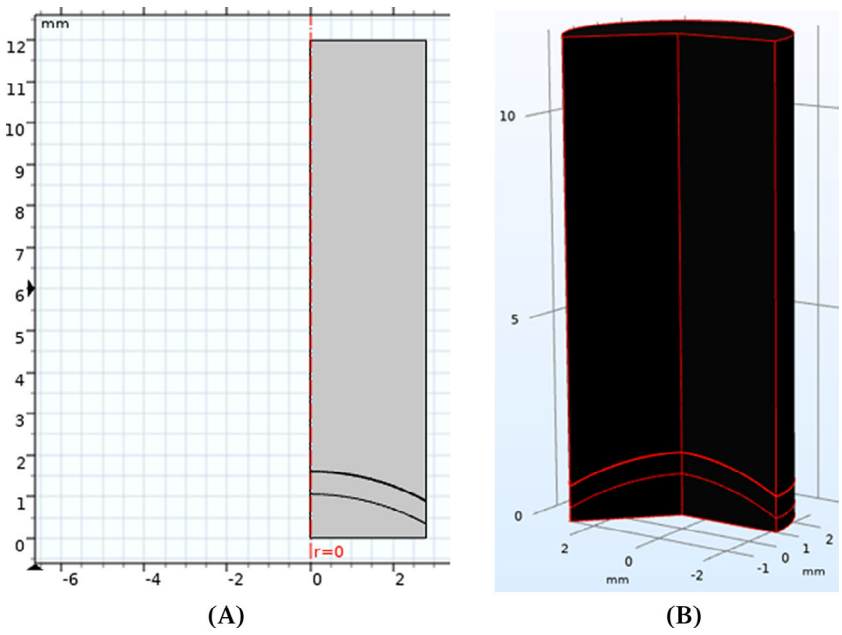

FIGURE 2 Setup and results for the simulations (A) 2D schematic of simulation model (B) 210° revolution of simulation model

The model was constructed as a half-body model to exploit the 2D axisymmetric nature of the human eye and reduce computational time.

Knowledge of accurate precorneal tear film thickness is limited, with no consensus on the true value. Invasive methods have produced estimates in the range 4 – 10 μm, this range is further supported by reflection spectra showing a peak at similar values.[29] Thus, the value of 5 μm was estimated. Precorneal tear film structure consists of an inner mucus layer and an outer oily layer; however, the structure is dominated by the middle aqueous layer which is mostly water and dissolved nutrients.[30] Therefore, for the simulation, the precorneal tear film layer was modeled as a water layer using the embedded software properties for water at room temperature.

As the geometry is curved, a perfectly matched layer could not be utilized to represent the open space. Thus, the boundaries were modeled as artificial boundary layers to simulate an open cavity as they do not represent physical walls.

The sound waves can be assumed as high frequency (≥2000 Hz) and highly localized due to the production of the sound wave from a local source. With these conditions, the sound source can be modeled as a Gaussian pulse (a pulse with the temporal shape of a Gaussian distribution) of 1 mm radius.[31,32] The use of a high frequency sound nullifies the material thickness effect on absorption that affects low frequency incident sound waves.[32] The incident pressure field was defined as cylindrical wave radiation as this allows the pressure wave to leave the domain without spurious reflections based on the conditions of the simulation.[33] During the simulation, the sound waves will be reflected off the center of the cornea, thus a constant corneal thickness is assumed, although in reality, the thickness increases toward the periphery.[34] In addition, it also assumed that there will be no reflection from the retina, isolating the reflections from the cornea.

Using the acoustics module within COMSOL Multiphysics, IOP could not be explicitly input as a parameter, thus, the relationship between IOP and a physical parameter that exploits the governing equations of the Pressure Acoustics, Frequency Domain was established.[35]

Previous experiments for a wide range of applications have estimated the porosity of a material using its pressure, as in a lot of cases it is easier to measure pressure variations in changing conditions. As a result of this,

many have formulated relationships estimating the porosity of a material using pressure, showing there is a relationship between the two parameters.[36-39] Porosity is a parameter that can be explicitly used as a dependent variable in COMSOL Multiphysics, thus it can be used to prove an implicit relationship between pressure and reflection coefficient.

Porosity is a value between 0 and 1 that represents a fraction of the volume of pores in a material compared to total mass volume, usually ranging up to a maximum value of over 0.5 for peat or clay.[40] For this reasoning, the porosity values were ranged from 0.1 to 0.6 to verify the relationship between porosity and reflection coefficient. Parameters input into COMSOL Multiphysics are outlined in Table 2.

2.2 | Results

The geometry and parameter set up allowed an accurate model to be created and allowed a sweep of frequency and porosity. This was used to obtain results confirming the relationship between pressure and reflection coefficient. The results are shown in Figure 3.

Figure 3 shows that at lower frequencies (<6000 Hz) the reflection coefficient shows a positive correlation with the material's porosity, and thus the pressure. A porosity value of 0.2 showed an anomaly at a frequency of 2000 Hz with a largely inflated value, likely due to inaccuracies of the modeling software at lower frequencies. As the frequency was increased in the range 6000 – 20,000 Hz, the reflection coefficient converged to a reflection coefficient of 0, rendering these frequencies useless for experimentation. Due to the convergence to 0, Figure 3 only shows the results up to 16,000 Hz. Figure 3 shows that the most variation in reflection coefficients between porosity values is evident at a driving frequency of 4000 Hz, and thus, this will be investigated further. Figure 4 shows the relationship between porosity and reflection coefficient at a driving frequency of 4000 Hz, showing a significant positive correlation.

This confirms the relationship between IOP and reflection coefficient, validating the worthiness of conducting the experiment. It can be conceded that the quality of the results shown in Figure 3 are not excellent, due to the convergence of the results and the variation in relationships shown at different porosities. However, due to Figure 4 showing a very clear relationship, this was considered as justification to conduct the physical experimentation.

TABLE 2 COMSOL multiphysics input parameters

Parameter	Value
Driving frequency sweep	2000 – 20,000 Hz in 1000 Hz increments
Corneal porosity sweep	0.1 – 0.6 in 0.1 increments
Density	1050 kg m^{-3}[41,42]
Permeability	1.361×10^{-11}[43,44]
Youngs Modulus	0.208 MPa[45]
Poisson ratio	0.49[46]
Bulk modulus	3.47×10^{6} Pa[47]
Shear modulus	6.98×10^{4} Pa[47]

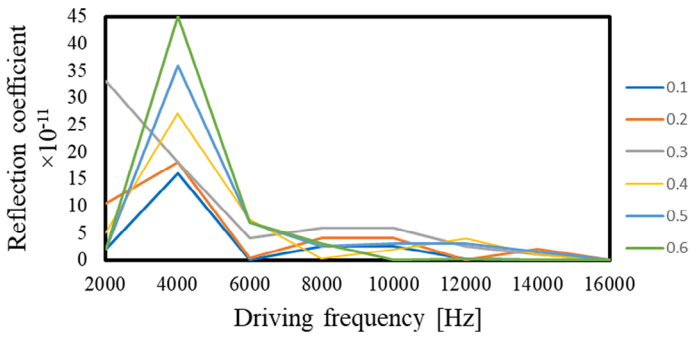

FIGURE 3 Graph of reflection coefficient vs driving frequency for porosity 0.1–0.6

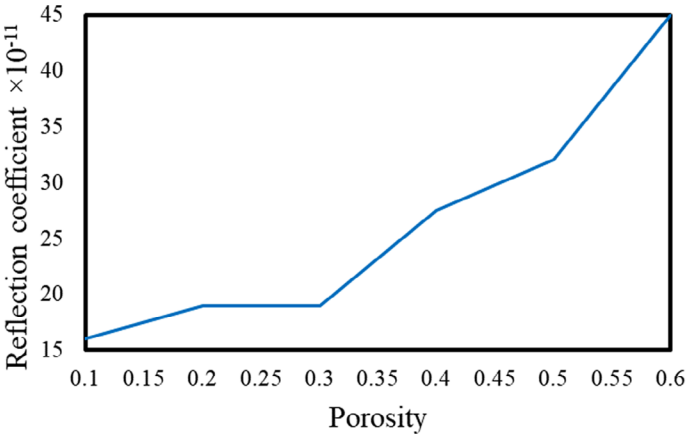

FIGURE 4 Graph of reflection coefficient vs porosity at a driving frequency of 4000 Hz

3 | PHYSICAL TESTING

3.1 | Theory

To investigate the relationship between IOP and the reflection coefficient, an experiment was conducted. The experiment involved the application of the hydrostatic pressure theory to determine the pressure inside an object replicating the human eye. Hydrostatic pressure is defined as "The pressure exerted by a fluid at equilibrium at a given point within the fluid, due to the force of gravity. Hydrostatic pressure increases in proportion to depth measured from the surface because of the increasing weight of fluid exerting downward force from above."[48] It follows the relationship shown by Equation (1).

$$p = \rho g h^{[39]} \tag{1}$$

Where
P = pressure in liquid at depth h [Pa],
ρ = density of fluid (water) = 1000 kg m^{-3},
g = gravitational constant = 9.81 m s^{-2},
h = depth in fluid [m].

97.5% range of human eye pressure varies between 7.3 and 22.1 mmHg,[49] equating to approximately 950 – 2950 Pa. Solving for h (Equation (1)), this is a variation in depth of approximately 0.10 – 0.30 m. The measurement at a water depth of 0.30 m represents the reading of an eye with ocular hypertension.

Sound waves fired at the eye will experience a portion of the wave that will aim to pass through the medium, whereas the remaining wave energy will reflect off the medium at an angle equal to the angle of the incident wave, as illustrated by Figure 5.[50] The reflection coefficient of the medium is defined as the ratio of the reflected wave to incident wave amplitudes and is a relationship commonly exploited in ultrasound applications.[51]

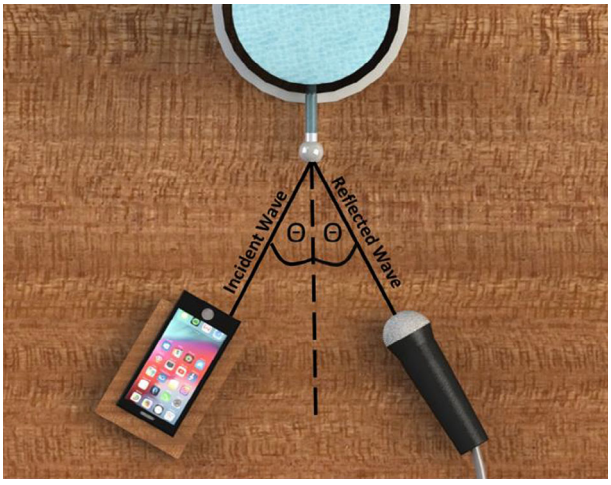

FIGURE 5 Incident versus reflected wave angle schematic

The material properties for the eye replicating object in the experimental method will dictate the resonant frequency of the object. At resonance, the absorption of the material is maximum and the reflection coefficient will become problematic to analyze.[52] For these reasons, an initial frequency sweep was performed at a constant pressure to identify the resonant frequency of the object and ensure it is avoided in further experimentation.

The geometry of incident surfaces is exploited in acoustics in conjunction with material properties to significantly alter the reflection of sound waves in applications such as soundproofing rooms and optimizing sound quality in recording studios. Therefore, it is essential that the geometry of the replica eye remains constant throughout the experimentation to nullify the effect.

3.2 | Experimental method

The depth of water was varied using a graduated water tower with a nozzle at the lower end for attachment of the replica eye shown in Figure 6.

The replica eye used was a latex balloon housed in plastic tubing, due to its benefit of retaining its geometry with varying levels of pressure. Sound waves were generated using a smartphone (iPhone 8) application 'Tone generator', with the lower right speaker being isolated for the experiment.[53] A Zoom U-44 Handy Audio Interface and an sE SE1A microphone were used in conjunction with computer software Audacity as an oscilloscope to analyze the sound waves. Images of the equipment used are shown in Figure S2. The equipment was set up as shown in Figure 5, ensuring the reflected wave is directed toward the center of the microphone. Figure 7(A),(B) shows further views of the apparatus setup.

The sound wave source and microphone were both placed a distance of at least one wavelength away from the reflection boundary, which is a distance of 0.172 m for the minimum frequency of 2000 Hz, using Equation (2).

$$\lambda = \frac{c}{f} \tag{2}$$

Where
λ = wavelength [m],
c = speed of sound at sea level =344 m s^{-1},
f = frequency [Hz].

To conduct the experiment, the sound wave was exposed to the material for approximately 2 s. This allowed ample time for Audacity to provide a stabilized sound pattern for analysis.

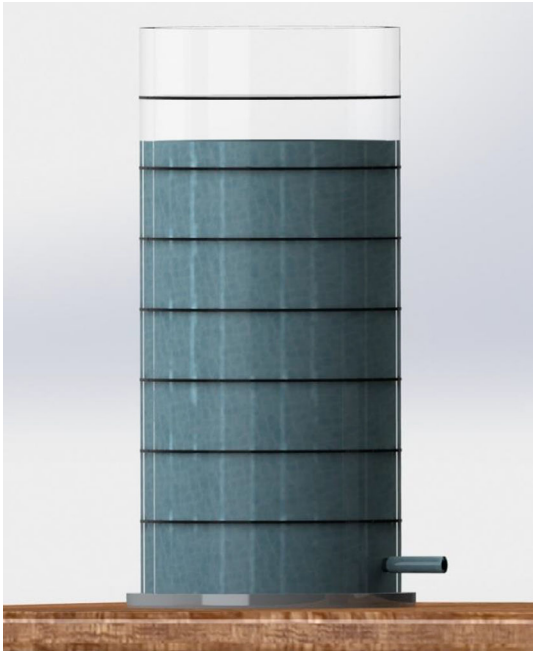

FIGURE 6 Side profile of water tower

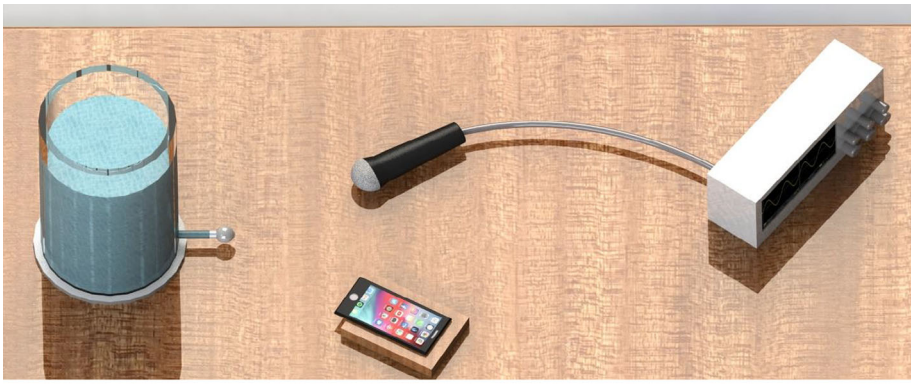

(A)

(B)

FIGURE 7 Schematics of the experimental setup produced on SolidWorks (A) Diagonal view of the experimental setup, (B) approximate human perspective of experimental setup

The frequency sweep was conducted by increasing the frequency from 2000 to 16,000 Hz in 1000 Hz increments. The results of the peak amplitude at the driving frequencies are shown in Table 3. The sweep was conducted using an incident wave angle (θ) of 30° and a water depth (h) of 0.175 m.

The internal pressure of the replica-eye was increased by increasing the water depth from 0.10 to 0.30 m in 0.025 m increments. The incident wave angle was again set at 30°. The results are shown in Table 5.

3.3 | Results and discussion

Figure 8(A) shows the frequency spectrum produced on Audacity for a driving frequency of 2000 Hz. The subsequent peaks after the largest at 2000 Hz are all at intervals of 2000 due to the waves being harmonics of each other, shown by Figure 8(B). This shows the first seven harmonics, which for the 2000 Hz incident wave frequency represents the peaks up to and including 14,000 Hz.

This confirms that Figure 8(A) matches the theoretical frequency spectrum for an incident wave frequency of 2000 Hz, and this trend continues for all frequency analysis conducted on Audacity. It is confirmed from this that there was negligible background noise interference in any of the sound recordings during the experiments. Figure 8(A) also confirms the accuracy of the application used to generate the sound waves, 'Tone generator'.

Table 3 shows the results for the frequency sweep and is illustrated by Figure 9.

From these results it can be concluded that the resonant frequency for the replica eye is at 11,000 Hz and the optimal frequency for maximizing reflection is 8000 Hz. The results confirm the theoretical pattern, where there is a frequency (11,000 Hz) which represents the resonant frequency of the material and absorption increases to a much higher value than at surrounding frequencies. There is also a frequency (8000 Hz) where reflection is maximum, matching theoretical expectations. For these reasons, the results from the initial frequency sweep can be assumed as accurate.

TABLE 3 Driving frequency versus peak sound level

Driving frequency (Hz)	Sound level (dB)
2000	−33.5
3000	−35.0
4000	−33.5
5000	−41.0
6000	−38.3
7000	−30.5
8000	−21.7
9000	−26.6
10,000	−35.0
11,000	−56.8
12,000	−37.7
13,000	−39.1
14,000	−37.2
15,000	−41.8
16,000	−49.1

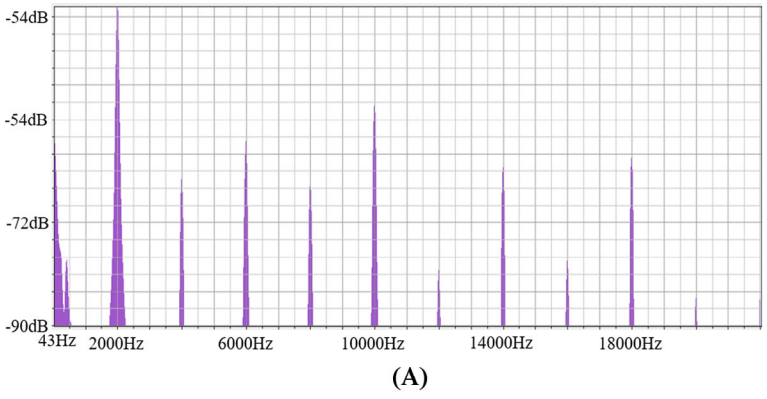

FIGURE 8 (A) Frequency spectrum for 2000 Hz produced on Audacity, (B) harmonic nodes of sound waves

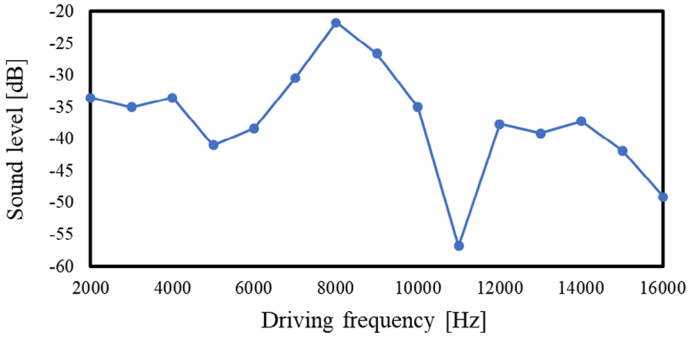

FIGURE 9 Sound level versus driving frequency graph

With the optimal driving frequency determined, the incident wave amplitude was determined by firing an 8000 Hz sound wave directly at the microphone at the same distance as the reflected waves, resulting in a sound level of −16.6 dB. Supplementary results used to calculate an average for calculations to populate Table 5 are shown in Table 4. The standard deviation values provide an indication to the spread of the data, relatively low in this experiment. The standard deviations are increased by relatively higher values for all readings in the first completion of the experiment, shown in Table 4. However, all of the completions of the experiment showed the same relationship, so the elevation of the first set was considered as unimportant in the context of the experiment.

The reflection coefficients in Table 4 were calculated using Equation (3).

$$R_C = \left(\frac{A_R}{A_I}\right)^{-1} = \frac{A_I}{A_R} \tag{3}$$

Where

R_C = reflection coefficient,

A_R = average sound level of reflected wave (Table 4),

A_I = sound level of incident wave= −16.6 dB.

Note the sound level values in Audacity are negative as the reference is a zero value, representing the maximum sound level possible for analysis on Audacity before distortion. This is the reason for Equation (3) being inverted, with its more common form being applicable to positive values of sound level. The data in Table 5 is illustrated in Figure 10.

The results show that as the internal pressure of an object increases, the reflection coefficient increases. Initially the increase shows a linear fashion, at a rate of approximately 1.80 R_C. $mmHg^{-1}$ through the range $0.100 - 0.200$ m, however this rate decreases and begins to plateau as the pressure increases above a depth of 0.250 m. It can be comprehensively concluded from this that there is a relationship between internal pressure of an object and its acoustic reflection

TABLE 4 Depth of water versus reflection coefficients for a driving frequency of 8000 Hz

Height of water (m)	Sound level 1 (dB)	Sound level 2 (dB)	Sound level 3 (dB)	A_R (dB)
0.100	−27.7	−25.2	−24.5	-25.8 ± 1.7
0.125	−25.6	−23.9	−23.3	-24.3 ± 1.2
0.150	−23.4	−22.6	−23.0	-23.0 ± 0.4
0.175	−21.8	−21.8	−20.6	-21.4 ± 0.7
0.200	−21.4	−19.2	−19.6	-20.1 ± 1.2
0.225	−20.0	−18.7	−19.2	-19.3 ± 0.7
0.250	−19.4	−18.6	−18.7	-18.9 ± 0.4
0.275	−19.1	−18.4	−18.9	-18.8 ± 0.4
0.300	−18.7	−18.4	−18.5	-18.5 ± 0.2

TABLE 5 Depth of water vs average reflection coefficient for a driving frequency of 8000 Hz

Depth of water (m)	Pressure (Pa)	R_C
0.100	981	0.65
0.125	1226	0.68
0.150	1472	0.72
0.175	1717	0.78
0.200	1962	0.83
0.225	2207	0.86
0.250	2425	0.88
0.275	2698	0.88
0.300	2943	0.90

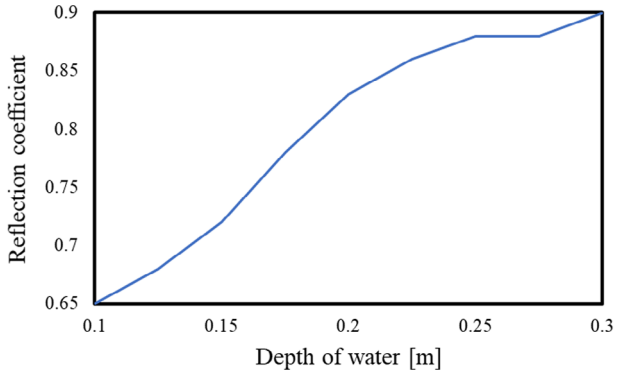

FIGURE 10 Reflection coefficient versus water depth at 8000 Hz driving frequency graph

coefficient, when other parameters are kept constant. Although this confirms there is a relationship, being able to accurately measure IOP using sound waves from a mobile device may prove difficult due to the relatively small increase in R_C for the increase in IOP. It could however be very useful in the monitoring of an individual's IOP and flag up when the individual experiences an increase in IOP if it were to be monitored consistently over a period of time.

The reflection coefficients shown in Table 5 may be inflated as there was nothing preventing some soundwaves traveling directly from the source, to the microphone without reflecting off the object. As the sound level of the source and the positioning of the source and microphone were invariable, it was assumed that the inflation as a result of this would be the same for all readings of wave amplitude. Thus, it would not cause a misinterpretation of the relationship.

Following on from the results of this experiment, it is evident that the plateauing of results occurs toward the pressure range indicating hypertension in a patient's eyes. As this could be due to the relatively larger values of reflection coefficient at a driving frequency of 8000 Hz, shown in Figure 9, a further experiment was conducted at a driving frequency of 6000 Hz to investigate if this would avoid, or delay, the plateauing effect. The experiment was conducted in an identical manner to the experiment previous, apart from the change to the driving frequency and the depth of water range was increased to $0.10 - 0.40$ m to investigate the pressures beyond ocular hypertension. The baseline sound level recorded was -16.0 dB. The associated results are given in Tables 6 and **7**, and the reflection coefficient vs depth of water graph is shown in Figure 11.

As can be seen from these results, the same relationship is shown, with an increase in internal pressure causing an increase in reflection coefficient. The plateauing effect is delayed to values beyond those indicative of ocular hypertension, however the gradient of the relationship is smaller than previous. As the measurement of discrete differences in IOP was already a concern, this further reduction may render accurate measurements unattainable by individuals. Figure 12 shows a graph comparing the reflection coefficient of the sound waves for both incident wave frequencies of 6000 and 8000 Hz.

TABLE 6 Depth of water vs reflection coefficients for a driving frequency of 6000 Hz

Height of water (m)	Sound level 1 (dB)	Sound level 2 (dB)	Sound level 3 (dB)	A_R (dB)
0.100	−46.4	−52.3	−51.3	-50.0 ± 2.6
0.125	−42.6	−48.0	−46.4	-45.7 ± 2.3
0.150	−39.9	−43.9	−40.6	-41.5 ± 1.7
0.175	−36.0	−39.2	−36.5	-37.2 ± 1.4
0.200	−34.1	−36.5	−33.9	-34.8 ± 1.2
0.225	−32.1	−34.5	−32.0	-32.9 ± 1.2
0.250	−30.5	−32.9	−31.3	-31.6 ± 1.0
0.275	−28.7	−32.8	−30.9	-30.8 ± 1.7
0.300	−28.2	−30.4	−30.0	-29.5 ± 1.0
0.325	−28.8	−29.8	−28.8	-29.1 ± 0.5
0.350	−28.1	−29.0	−28.6	-28.6 ± 0.4
0.375	−27.8	−28.4	−28.2	-28.1 ± 0.2
0.400	−27.8	−28.2	−28.0	-28.0 ± 0.2

Depth of water (m)	Pressure (Pa)	R_C
0.100	981	0.32
0.125	1226	0.35
0.150	1472	0.39
0.175	1717	0.43
0.200	1962	0.46
0.225	2207	0.49
0.250	2425	0.51
0.275	2698	0.52
0.300	2943	0.54
0.325	3188	0.55
0.350	3434	0.56
0.375	3679	0.57
0.400	3924	0.57

TABLE 7 Depth of water vs average reflection coefficients for a driving frequency of 6000 Hz

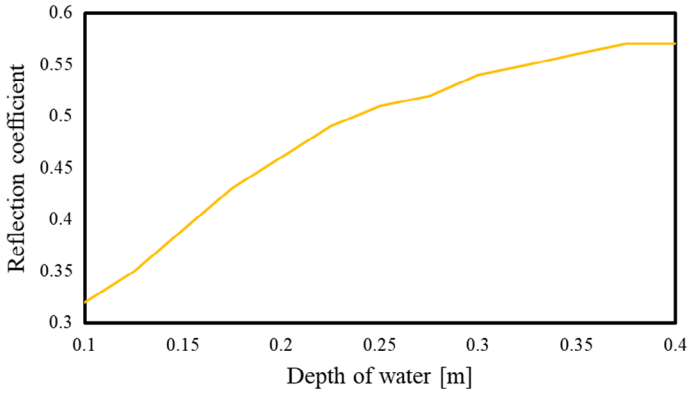

FIGURE 11 Reflection coefficient vs water depth at 6000 Hz driving frequency

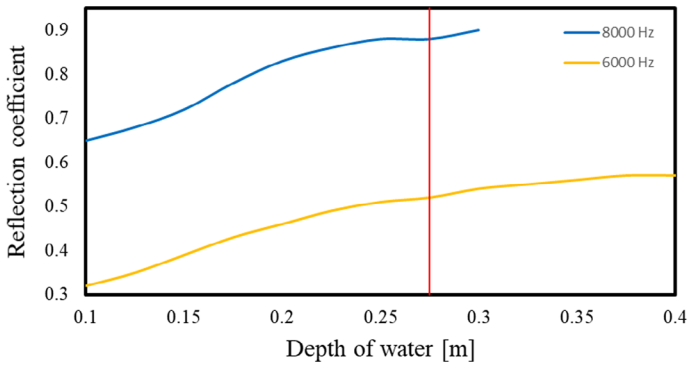

FIGURE 12 Reflection coefficient vs water depth comparison between 6000 and 8000 Hz driving frequency

The red line represents the depth of water indicating ocular hypertension, 0.285 m. This value was calculated using Equation (1) and a pressure value of 22.1 mmHg (2800 Pa).[12] Figure 12 clearly shows the delay in the plateauing of results past the hypertension indicative red line for a 6000 Hz driving frequency. However, as previously discussed, despite delaying a complete plateauing, the increase in reflection coefficient may not be sufficient to be accurately measurable.

In addition, sensitivity in the range higher than 29 mmHg (~0.4 m depth) is required in clinical practice. As discussed, there is a plateauing of results as the pressure is increased in to these ranges, and it may be as a consequence that sensitivity in the desired range is not achievable. However, using this method as a mobile indicator of increasing eye pressure, and the need for the individual to get further testing done is still a viable application of the theory.

3.4 | Limitations and outlook

The preliminary nature of these findings should be noted here, with this stand-alone experiment not being enough to constitute a confirmation that the application of the theory would work. Experiments must be completed to confirm the relationship, if any, that acoustic reflection coefficient has with CCT which would allow this method to stand out amongst competing methods. The geometry of the eye's effect on readings must also be quantified through experimentation, where there is a risk that the adverse effects may be too great for the method described to be achievable. It is perceived that apart from the stiffness of the ocular surface, the corneal conditions may also cause the sound reflections to vary. It should also be noted that the soundwaves used in the experiments do produce audible sounds, some of which may cause discomfort to the patient. For this reason, once ethics have been obtained to conduct the experiment on live patients, the use of ear plugs may be required. This may then reduce the accessibility of the method to an individual, as access to ear plugs, if required, would be assumed.

Currently there are no experiments underway investigating the factors outlined above, which is essential for this to be considered a viable method of measuring a patients IOP.

4 | CONCLUSION

In conclusion, a relationship was confirmed between internal pressure and acoustic reflection coefficient. The aim was met comprehensively through physical experimentation, which showed a clear increase in the reflection coefficient as the internal pressure of an object increased at a rate that is measurable for mobile equipment. Critical frequencies were also discovered for effective measurement of reflection coefficient at pressure values that surpass those of ocular hypertension. In practice, the critical frequency value for human eyes must be determined through experimentation using a method similar to that completed in this report and analyzed for suitability.

Although the relationship confirmed achieved the aim of the project, the investigation was performed whilst keeping other material properties consistent, most notably the geometry of the object. Geometry is a property that is different for all individuals and is also a property that has a significant effect on sound wave reflections. Thus, it is probable that sound waves could accurately be used to measure IOP if the geometry of the eye is known. Further investigation should be conducted into the accurate, mobile measurement of eye geometry, rendering a complete eye pressure measurement achievable. For this to be an accurate measurement, an investigation should be conducted to quantify the changes in eye geometry and how this impacts the value of the reflection coefficient. If this is achieved, it is fully viable for an accurate, mobile measurement of IOP to be conducted using a smartphone, from the comfort of the user's home.

PEER REVIEW INFORMATION

Engineering Reports thanks the anonymous reviewers for their contribution to the peer review of this work.

PEER REVIEW

The peer review history for this article is available at https://publons.com/publon/10.1002/eng2.12355.

DATA AVAILABILITY STATEMENT

The data that support the findings of this study are available from the corresponding author upon reasonable request.

CONFLICT OF INTEREST

The authors declare that there is no conflict of interest regarding the publication of this article.

ORCID

Matthew Soanes https://orcid.org/0000-0003-0151-1892

REFERENCES

1. Semeraro F, Cancarini A, dell'Omo R, Rezzola S, Romano M, Costagliola C. Diabetic retinopathy: vascular and inflammatory disease. *J Diabetes Res*. 2015;2015:1-16.
2. Killer HE, Miller NR, Flammer J, et al. Cerebrospinal fluid exchange in the optic nerve in normal-tension glaucoma. *Br J Ophthalmol*. 2012;96:544-548.

3. Berdahl JP, Allingham RR. Intracranial pressure and glaucoma. *Curr Opin Ophthalmol*. 2010 Mar;21(2):106-111. https://doi.org/10.1097/ICU.0b013e32833651d8.
4. Roy Chowdhury U, Fautsch MP. Intracranial pressure and its relationship to Glaucoma: current understanding and future directions. *Med Hypothesis Discov Innov Ophthalmol*. 2015;4(3):71-80.
5. Kharmyssov C, Abdildin YG, Kostas KV. Optic nerve head damage relation to intracranial pressure and corneal properties of eye in glaucoma risk assessment. *Med Biol Eng Comput*. 2019;57:1591-1603.
6. MedicineNet. Medical definition of intraocular pressure. https://www.medicinenet.com/script/main/art.asp?articlekey=4014. Accessed September 2019.
7. Wang YX, Xu L, Wei WB, Jonas JB. *Intraocular pressure and its normal range adjusted for ocular and systemic parameters. The Beijing Eye Study 2011*. 2018;13(5).
8. Tham Y-C, Li X, Wong TY, Quigley HA, Aung T, Cheng C-Y. Global prevalence of Glaucoma and projections of Glaucoma burden through 2040. *Ophthalmology*, *ISSN: 1549-4713*. 2014;121(11):2081-2090.
9. BrightFocus Foundation. How is Eye Pressure Measured? BrightFocus Foundation. https://www.brightfocus.org/glaucoma/article/how-eye-pressure-measured#:~:text=Your%20ophthalmologist%20will%20instruct%20you,fixed%20area%20of%20the%20cornea. Accessed September 2019.
10. Shah S. Accurate intraocular pressure measurement-the myth of modern ophthalmology? *Ophthalmology*, ISSN: 0161-6420. 2000;107(10):1805-1807.
11. McMonnies CW. Glaucoma history and risk factors. *J Optom*. 2016;2017:71-78.
12. McCafferty S, Levine J, Schwiegerling J, Enikov ET. Goldmann applanation tonometry error relative to true intracameral intraocular pressure in vitro and in vivo. *BMC Opthalmol*. 2017;17(1):215.
13. Zadok D, Tran DB, Twa M, Carpenter M, Schanzlin DJ. Pneumotonometry versus Goldmann tonometry after laser in situ keratomileusis for myopia. *J Cataract Refract Surg*, ISSN: 0886-3350. 1999;25(10):1344-1348.
14. De Moraes CGV, Prata TS, Liebmann J, Ritch R. Modalities of tonometry and their accuracy with respect to corneal thickness and irregularities. *J Optom*. 2008;1(2):43-49.
15. Farhood QK. Comparative evaluation of intraocular pressure with an air-puff tonometer versus a Goldmann applanation tonometer. *Clin Ophthalmol.* 2013;7:23-27.
16. Sit AJ, Lin SC, Kazemi A, McLaren JW, Pruet CM, Zhang X. In vivo noninvasive measurement of Young's modulus of elasticity in human eyes: a feasibility study. *J Glaucoma*. 2017;26(11):967-973.
17. Zhou B, Chen JJ, Kazemi A, Sit AJ, Zhang X. An ultrasound Vibro-Elastography technique for assessing papilledema. *Ultrasound Med Biol*. 2019;45(8):2034-2039.
18. Essilor News. The eye air puff test – why you can't hide from it. https://www.essilorusa.com/newsroom/the-eye-air-puff-test-why-you-cant-hide-from-it. Accessed October 2019.
19. Glaucoma NZ. Your Glaucoma Eye Examination: Part 1. *Your Eye Pressure*. 2008 *Vol:* 5*, Issue:* 1.
20. Iliev ME, Goldblum D, Katsoulis K, Amstutz C, Frueh B. Comparison of rebound tonometry with Goldmann applanation tonometry and correlation with central corneal thickness. *Br J Ophthalmol*. 2006;90(7):833-835.
21. Nakakura S. Icare rebound tonometers: review of their characteristics and ease of use. *Clin Ophthalmol*. 2018;12:1245-1253.
22. NICE Pathways. Icare rebound tonometer to measure intraocular pressure. https://www.nice.org.uk/advice/mib57. Accessed October 2019.
23. Sutton B. Smartphone Tonometer Provides Reliable Preliminary IOP; 2020. https://www.healio.com/news/optometry/20200114/smartphone-tonometer-provides-reliable-preliminary-iop#.
24. Wu Y, Luttrell I, Feng S, et al. Development and validation of a machine learning, smartphone-based tonometer. *Br J Ophthalmol*. 2020;104:1394-1398.
25. Pew Research Centre. Mobile Fact Sheet. https://www.pewinternet.org/fact-sheet/mobile/. Accessed October 2019.
26. COMSOL Application Gallery. Acoustic reflection analyser for a water-sediment interface. https://uk.comsol.com/model/acoustic-reflection-analyzer-for-a-water-sediment-interface-30881. Accessed September 2019.
27. Rufer F, Schroder A, Erb C. White-to-white corneal diameter. *Cornea*. 2005;24(3):259-261.
28. Mashige K. A review of corneal diameter, curvature and thickness values and influencing factors. *African Vis Eye Health*. 2013;72(4):185–194.
29. Ewen King-Smith P, Fink B, Fogt N, Nichols K, Hill R, Wilson G. The thickness of the human Precorneal tear film: evidence from reflection spectra. *Investig Ophthalmol Vis Sci*. 2000;41:3348-3359.
30. Vismed.trbchemedica.co.uk. The precorneal tear film. https://vismed.trbchemedica.co.uk/business-professionals/understanding-the-tear-film/the-precorneal-tear-film. Accessed January 2020.
31. Weik M.H. Gaussian-shaped pulse. *Computer Science and Communications Dictionary*. Springer, Boston, MA. 2017 *Vol:* 2017*, Issue:* 1*, Page:* 676
32. Seddeq HS. Factors influencing acoustic performance of sound absorptive materials. *Australian J Basic Appl Sci*. 2009;3(4):4610-4617.
33. COMSOL. Theory for the plane, spherical, and cylindrical radiation boundary conditions. https://doc.comsol.com/5.5/docserver/#!/com.comsol.help.aco/aco_ug_pressure.05.130.html. Accessed January 2020.
34. Martola E. Central and peripheral corneal thickness. *Arch Ophthalmol*. 1968;79(1):28-30.
35. COMSOL. *Acoustic Module User's Guide*. Stockholm, Sweden: COMSOL; 2018. https://doc.comsol.com/5.4/doc/com.comsol.help.aco/AcousticsModuleUsersGuide.pdf. Accessed October 2019.

36. de Siqueira MF, Silva F, Marsili MD, Rocha PS, Kronbauer A, Sisk C, Grader A, Toelke J, Jordan A. Estimation of permeability, porosity and rock compressibility properties using digital rock analysis technique for a heavy oil unconsolidated sandstone offshore Brazil. Search and Discovery; 2018, Article #30587.
37. Ghabezloo S, Sulem J, Saint-Marc J. Evaluation of a permeability porosity relationship in a low permeability creeping material using a single transient test. *Int J Rock Mech Min Sci*. 2009;46(4):761-768.
38. Kitamura K, Takahashi M, Mizoguchi K, Masuda K, Ito H, Song S. Effects of pressure on pore characteristics and permeability of porous rocks as estimated from seismic wave velocities in cores from TCDP hole-a. *Geophys J Int*. 2010;182(3):1148-1160.
39. Glover P. Formation evaluation MSc course notes. http://homepages.see.leeds.ac.uk/~earpwjg/PG_EN/CD%20Contents/Formation%20Evaluation%20English/Chapter%205.PDF. Accessed December 2019.
40. Martin F, Colpitts R. Reservoir engineering. *Standard handbook of petroleum and natural gas engineering*. Vol 2. Texas, TX: Gulf Professional Publishing; 1996:1-362.
41. Shao P, Seiler T, Eltony A, Ramier A, Kwok S, Scarcelli GR II, Yun S. Effects of corneal hydration on Brillouin microscopy in vivo. *Investig Opthalmol Visual Sci*, 2018, *Vol:* 59*, Issue:* 7*, Page:* 3020
42. Leonard D, Meek K. Refractive indices of the collagen fibrils and extrafibrillar material of the corneal stroma. *Biophys J*. 1997;72(3):1382-1387.
43. Prausnitz M, Noonan J. Permeability of cornea, sclera, and conjunctiva: a literature analysis for drug delivery to the eye. *J Pharm Sci*. 1998;87(12):1479-1488.
44. Lee V. Mechanisms and facilitation of corneal drug penetration. *J Control Release*. 1990;11(1–3):79-90.
45. Shih P, Huang C, Huang T, et al. Estimation of the corneal Young's modulus in vivo based on a fluid-filled spherical-Shell model with Scheimpflug imaging. *J Ophthalmol*. 2017;2017:1-11.
46. Aloy M, Adsuara J, Cerdá-Durán P, et al. Estimation of the mechanical properties of the eye through the study of its vibrational modes. *PLOS One*. 2017;12(9):e0183892.
47. Bower, A. Constitutive models- relations between stress and strain. *Appl Mech Solids*. 2008;1(1):1–1. http://solidmechanics.org/text/Chapter3_2/Chapter3_2.htm.
48. Dictionary.com. Definition of hydrostatic pressure. https://www.dictionary.com/browse/hydrostatic-pressure. Accessed January 2020.
49. Wang YX, Xu L, Wei WB, Jonas JB. Intraocular pressure and its normal range adjusted for ocular and systemic parameters. The Beijing Eye Study 2011. *PLOS ONE*. 2018;13(5):e0196926. https://dx.doi.org/10.1371/journal.pone.0196926.
50. Bouzidi Y, Schmitt D. Incidence-angle-dependent acoustic reflections from liquid-saturated porous solids. *Geophys J Int*. 2012;191(3):1427-1440.
51. Dukhin A, Goetz P. Fundamentals of acoustics in homogeneous liquids. *Characterization of Liquids, Nano- and Microparticulates, and Porous Bodies Using Ultrasound*. Vol 24. Amsterdam: Elsevier; 2010:91-125.
52. Schwan L, Umnova O, Boutin C. Sound absorption and reflection from a resonant metasurface: homogenisation model with experimental validation. *Wave Motion*. 2017;72:154-172.
53. App Store. Tone generator; 2011. https://apps.apple.com/gb/app/tone-generator/id457003837. Accessed February, 2020.

SUPPORTING INFORMATION

Additional supporting information may be found online in the Supporting Information section at the end of this article.

How to cite this article: Soanes M, Essa K, Butt H. Testing the viability of measuring intraocular pressure using soundwaves from a smartphone. *Engineering Reports*. 2021;e12355. https://doi.org/10.1002/eng2.12355